

Revealing of sources of atmospheric aerosol pollution from data of remote sensing and back-trajectory statistics

V.P. Kabashnikov,¹ V.N. Kuz'min,² A. Pietruczuk,³
P. Sobolewski,³ and A.P. Chaikovskii¹

¹*Institute of Physics, Belarus National Academy of Sciences, Minsk, Belarus*

²*ECOMIR Republican Scientific and Technical Center, Minsk, Belarus*

³*Institute of Geophysics, Warsaw, Poland*

Received May 2, 2007

The total aerosol content in the vertical atmospheric column was measured in Minsk (Belarus) and Belsk (Poland) with a multiwavelength aerosol lidar and a sun-scanning spectral radiometer. Three-dimensional five-day backward trajectories were calculated using wind field data of the HidroMetCenter of the Republic Belarus supplemented with the vertical wind velocity data and the data on the wind field in the atmospheric boundary layer. It was found that the most powerful aerosol source areas lie beyond the Belarus and Poland territories. They are situated south-east, south, and south-west from the monitoring stations. The revealed sources are close to the expert EMEP emission data. On the average, south territories affect mostly the atmospheric situation at the monitoring sites. About 60% of aerosols in Minsk and about 50% of aerosols in Belsk are of transborder origin.

Introduction

Atmospheric aerosol is among important factors determining the regional ecological situation. Owing to large-scale wind transport, not only local, but also remote aerosol sources can contribute significantly to aerosol pollution of the atmosphere. The location and parameters of aerosol pollution sources are often unknown. This is especially true for natural aerosol sources, as well as sources located at territories of foreign countries.

To find areas being stationary sources of air-transported aerosol, the so-called residence time analysis proposed for the first time in Refs. 1 and 2 is used. Input data for this method are data of pollutant content monitoring for a long time (for example, a year or several years) and a set of back trajectories of air masses incoming to the monitoring site at the time of concentration measurements. It is assumed that the air mass going at a rather low height (mostly within the atmospheric boundary layer) over a territory being an emission source entrains a pollutant and carries it, thus decreasing its concentration due to diffusion, deposition, and chemical transformations.

Using statistical processing of monitoring data and back trajectories, we can find correlations between the pollutant concentration at a monitoring site and territories, air masses went over before incoming at the monitoring site, and thus reveal the regions causing the increased pollutant concentration at the monitoring site.

In the considered method, the geographic area, back trajectories pass over, is divided into cells by a computational grid. The probability that some trajectory passes over a cell was calculated^{1,2} under the condition that at a monitoring site the pollution

level exceeds the average one. Cells with a high probability of the situation were identified as a source. In the following papers, the mean concentration³ at a monitoring site or the mean logarithm of the concentration⁴ were calculated under the condition that a trajectory passes over the given cell. Cells with the high concentration were considered as probable sources. In Ref. 5, the method of concentration redistribution along a trajectory, which more accurately locates a source, was proposed. The above described methods were used to reveal regions being sources of sulfur oxides,^{2,5,6} nitrogen oxides,⁶ ozone,⁷ acid precipitations,⁸ aerosols,⁴ and sources and sinks of CO₂ [Ref. 9] and radioactive ⁷Be [Ref. 10].

This paper presents the results of identification of sources of aerosol pollution of the atmosphere in Minsk and Belsk (Poland, 80 km from Warsaw) obtained from the data of remote lidar and radiometric monitoring of aerosol and back trajectory statistics with the use of the method from Ref. 3. The data of remote measurements contain the information about aerosol in the whole atmospheric column and, in particular, in the lower troposphere, where the large-scale transport of aerosol particles mostly occurs. These data are less subjected to influence of local aerosol sources than data of ground-based measurements. Therefore, in the problem of reconstruction of the large-scale spatial distribution of aerosol sources, the data of remote measurements have an advantage over the data of ground-based measurements.

Basic equations

Let $c(l)$ be the pollutant concentration measured at a monitoring site (receptor) at the time of arrival of the l th trajectory, and $\tau_{ij}(l)$ be the time of

residence of the l th trajectory over the territory of the (i, j) cell, indices i, j enumerate geographic coordinates (longitude and latitude) of the center of a selected cell. We assign the average concentration P_{ij} to every cell (i, j) at the receptor under the condition that the trajectory passes over the considered cell:

$$P_{ij} = \frac{\sum_{l=1}^N c(l)\tau_{ij}(l)}{\sum_{l=1}^N \tau_{ij}(l)}, \quad (1)$$

where N is the total number of back trajectories. The concentration P_{ij} characterizes the degree of potential influence of the cell on the pollutant content at the receptor. The actual contribution of the cell averaged for a long time to the average concentration at the receptor is characterized by the parameter F_{ij} , which is a product of the power P_{ij} by the probability W_{ij} of the trajectory passing over the cell (i, j) :

$$F_{ij} = W_{ij}P_{ij}, \quad (2)$$

where the probability W_{ij} of the trajectory passing over the cell (i, j) is the time of its residence in the cell (i, j) divided by the total time of its residence in all regions, back trajectories passed over:

$$W_{ij} = \frac{\sum_{l=1}^N \tau_{ij}(l)}{\sum_{ij} \sum_{l=1}^N \tau_{ij}(l)}. \quad (3)$$

The sum of contributions of all cells gives the average concentration at the receptor:

$$\sum_y F_{ij} = \frac{1}{N} \sum_{l=1}^N c(l). \quad (4)$$

The probability of pollutant capture is the highest at the altitudes, where the pollutant concentration is maximal. The experiment^{11–13} shows that most amount of aerosols are concentrated in the lower 2-km atmospheric layer, mostly within the atmospheric boundary layer (ABL). In addition, the lifetime of an aerosol particle is restricted by dry and wet sedimentation processes. This circumstance (along with the geometric factor) determines the weak influence of remote sources on the state of the atmosphere at a monitoring site. To take into account the most capture of pollutants from ABL and to restrict the influence of remote sources, we shall use instead the residence time of the trajectory over a cell, the effective residence time equal to the residence time multiplied by the weighting function:

$$g = \exp(-h/h_B)\exp(-t/t_E), \quad (5)$$

where h and h_B are the height of the trajectory and the ABL altitude; t and t_E are the time of air mass motion from the cell to the measurement site and the lifetime of an aerosol particle.

The ABL altitude varies from day to night and experiences seasonal variations. According to the data of Ref. 14, for conditions of the midland of Eastern

Europe the following ABL altitudes can be taken as typical: 700 and 300 m in the cold season and 1400 and 500 m, respectively, for day- and nighttime in the warm season. Then the altitude of the ABL upper boundary can be approximated by the following equations:

$$h_B = 725 + 225a + [325 + 125a]\sin(\pi/12(m-6)), \quad (6)$$

where

$$a = \sin[(2\pi/365)(d-356-19) + 3\pi/2]; \quad (7)$$

m is the local time, rounded to an hour, and indicating, when the air mass being at the measurement time at the monitoring site passed over the considered cell; d is the day number counted from the year beginning. Equation (7) takes into account the 19-day delay¹² of the average daily ABL altitude relative to the light day length.

Monitoring data and back trajectories

We used the data on the total content of the coarse and fine aerosol fractions in the vertical atmospheric column obtained with the aid of a multiwavelength aerosol lidar and an automated sun-scanning spectral radiometer¹³ at two sites of lidar monitoring: Minsk (Belarus) and Belsk (Poland). The fine fraction is understood as fine aerosol with the particle diameter not exceeding 2 μm . All particles of larger size were assigned to the coarse fraction. The period from October, 2004 to December, 2006 was under consideration. The data of more than 700 measurements for Minsk and more than 900 measurements for Belsk were used.

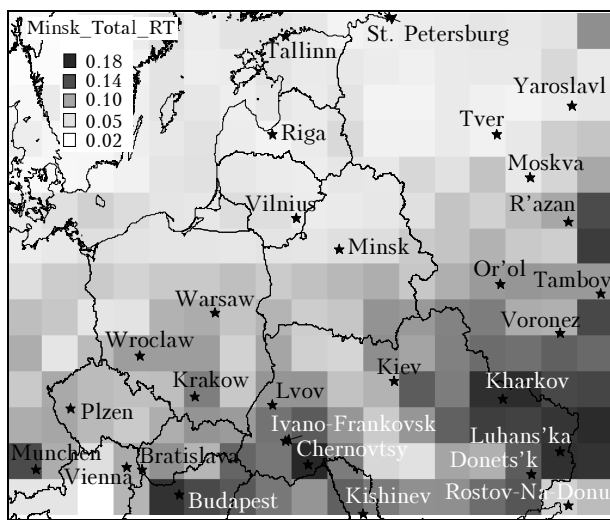
We calculated 5-day 3D back trajectories for the air mass arrival times coinciding with the measurement times, using the data of the Republic Belarus HidroMetCenter on horizontal wind and temperature field in the Northern Hemisphere. Wind fields were specified for 11 altitude levels up to 100 hPa, which roughly corresponded to an altitude of 16 km. The horizontal resolution of the wind field and temperature was 2.5 \times 2.5 $^\circ$. The temporal resolution of meteorological data was 12 h. The data of the Republic HidroMetCenter were supplemented with the data on the vertical wind component calculated from adiabatic measurements of temperature. In addition, parameterization^{15,16} was used to specify wind velocities inside ABL.

Since the most amount of aerosol was concentrated within ABL, lidar measurements were assigned to trajectories coming to the receptor point at two altitudes: 950 and 850 hPa, which roughly correspond to geometric altitudes of 450 and 1350 m. The relative contribution of each trajectory to the observed vertically integral pollutant content was assumed proportional to the effective residence time of the trajectory over all territories. The lifetime of coarse particles was estimated as a fall time of a particle of 10 μm in diameter from a height of 1 km. It turned

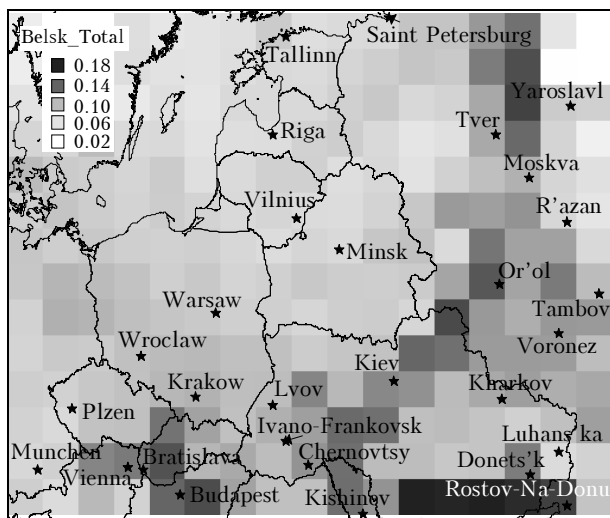
out to be 36 h. The lifetime of fine particles is determined by precipitation scavenging¹⁷ and was assumed to be 7 days in the calculations.

Calculated results

Figure 1 shows the concentration P_{ij} field calculated by Eq. (1) from the data on the total content of the fine and coarse aerosol in Minsk and Belsk. Cells with the high concentration were considered as probable sources. The cell size is 2° in longitude and 1° in latitude, which roughly corresponds to 133x100 km at the latitude of Minsk.



a



b

Fig. 1. Spatial density of power of total fine and coarse aerosol sources affecting the state of the atmosphere in Minsk (a) and Belsk (b).

For convenience, all figures show the same map fragment. Its dimensions are determined from the condition that no less than five trajectories cross every cell. As is seen, the most powerful sources of total dust lie beyond the territory of Belarus and

Poland to south-west, south, south-east, and east from the monitoring sites. For Minsk, it is the south-eastern border of Ukraine with Russia, Southern Carpathian region, and Hungary. Less powerful sources lie near Ryazan', Russian Black Earth Belt, Kiev, and south-eastern Germany. According to the data for Belsk, the most powerful sources lie at the south-eastern Ukraine–Russia border. Less powerful sources lie near Tver', at the north-eastern Ukraine–Russia border, in the Southern Carpathian region, Moldova, Hungary, and Slovakia. The main sources at the Belarus territory lie to the south of Minsk, and in Poland such sources lie at the central and southern parts.

The distributions of dust sources obtained from the data for Minsk and Belsk do not coincide, but have some common features. To find the degree of their quantitative closeness, we calculated the correlation

$$K_{12} = \sum_{i,j} p_{ij}^{(1)} p_{ij}^{(2)}, \quad (8)$$

where p_{ij} is the difference between the concentration P_{ij} in the (i, j) cell and the concentration averaged over the map fragment; superscripts 1 and 2 correspond to two monitoring sites, and summation in Eq. (7) is performed over cells on the map fragment. The correlation coefficient between the spatial distributions of total dust shown in Fig. 1 appeared to be 47%. Differences in the spatial distributions of sources may be connected with different conditions of air mass motion from sources to measurement sites, with possibly different flow movement conditions for Minsk and Belsk, as well as with insufficient accuracy of calculation of back trajectories and imperfection of the method.

The geographic distribution of power of total fine and coarse aerosol sources in 2004 according to the EMEP expert data^{18,19} is shown in Fig. 2.

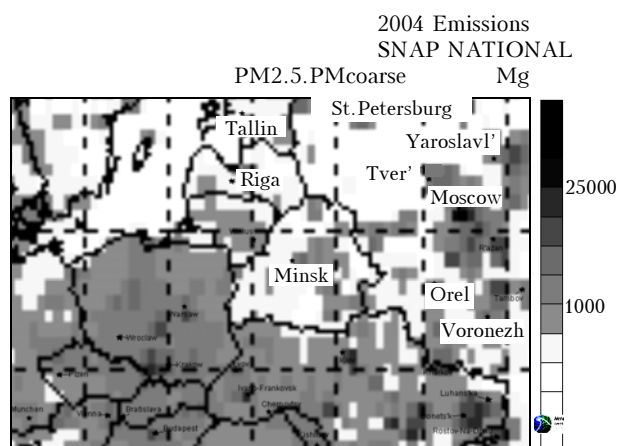


Fig. 2. Spatial distribution of power of total fine and coarse aerosol emission sources according to the EMEP data.

It can be seen that the dust sources within the regions covered by the map in Fig. 1 lie in southern and south-eastern Ukraine, south of the Carpathians,

in Moldova, Hungary, Slovakia, in southern and central Poland, near Moscow, north and south of Moscow, and in the Black Earth Belt of Russia. These regions are mostly shown in Fig. 1. The widest discrepancy between our and EMEP data is observed for the region of Moscow. Our calculation shows the presence of sources northward and southward of Moscow, but does not detect the cell containing Moscow. This is likely connected with inaccurate calculation of trajectories. In addition, in contrast to the EMEP data, our calculation gives no marked sources near Minsk. According to the data for Minsk, the cell containing Minsk is characterized as moderate in all concentration measurements. From the data for Belsk, some sources near Minsk were detected. This is likely also connected with poor trajectory calculations.

The actual influence of remote sources takes place rather rarely: only when air masses coming to monitoring sites previously cross source regions. On the average, for a year or several years the strongest (among territories of equal area) influence on the state of the atmosphere at monitoring sites is exerted by relatively close territories lying within 200–300 km from the monitoring sites. Nevertheless, the total influence of remote territories with the low density of the influence function can be significant. Thus, the ratio of the contribution from Belarus territories to the degree of atmospheric dust state in Minsk to the contribution from the entire territory covered by 5-day trajectories is roughly 30, 50, and 40%, respectively, for fine, coarse, and total aerosol. The ratio of the contribution from the Poland territory to the degree of atmospheric dustiness in Belsk to the contribution from the whole territory, covered by 5-day trajectories, is roughly 42, 61, and 50% for fine, coarse, and total aerosol, respectively. This means that, on average, about 60% of dust in the atmosphere of Minsk and 50% in the atmosphere of Belsk is of the transborder origin.

Table shows that major aerosol pollution contributors to the Minsk atmosphere are southern and eastern territories, and to Belsk atmosphere – southern and western territories. Northern territories are the smallest contributors to atmospheric pollution at the both monitoring sites.

Table. Relative contribution (%) of territories lying to east, north, west, and south of Minsk/Belsk to annual average aerosol pollution of the Minsk/Belsk atmosphere

Aerosol fraction	East	North	West	South
Fine+coarse	29/22	17/19	23/26	31/33
Fine	32/22	18/18	23/26	27/34
Coarse	25/22	16/21	22/25	37/32

To estimate the statistical reliability of the results obtained, the spatial distributions of sources were also calculated from the halved monitoring database with the use of only odd numbers of measurements. The results turned to be close to those shown in Fig. 1.

The correlation between the distributions obtained from the complete and halved databases is equal to 94% for Minsk and 96% for Belsk. This indicates that the monitoring database was sufficient for calculation of residence times. The accuracy of localization of pollutant sources is also connected with the accuracy of trajectory calculations. According to Ref. 20, the minimal calculation error achievable only for trajectories crossing ABL is 20% of the passed distance. The NASA²¹ and NILU²² back trajectories ending at Minsk were available for us. The NASA trajectories were calculated for the time of arrival of 0 and 12 GMT and the NILU trajectories were calculated for 0, 6, 12, and 18 GMT. First, we determined how our results changed when trajectories with actual times of arrival were replaced by trajectories with time of arrival at 0 and 12 GMT. The correlation coefficient of spatial distribution of sources determined for these two types of trajectories turned to be 81% for total dust.

The spatial distributions of sources of total dust obtained for our trajectories (OT) with times of arrival at 0 and 12 GMT and the NASA and NILU trajectories also with times of arrival at 0 and 12 GMT are characterized by the following levels of correlation: OT–NASA – 73%; NILU – 77%; NASA–NILU – 74%. Based on these estimates, we can believe that the correlation between the source distributions calculated from model and “actual” trajectories for the considered map fragment is about 75%.

Conclusions

Processing of remote monitoring and back trajectory data with the use of the residence time analysis has allowed us to reveal regions being sources of aerosol pollution of the atmosphere in Minsk and Belsk. The most powerful sources of total dust lie beyond territories of Belarus and Poland: they are located to south-west, south, and south-east from the monitoring sites. These results are mostly in agreement with the EMEP expert data. Major contributors to aerosol pollution of the Minsk atmosphere are southern and eastern territories, while for Belsk – southern and western ones. On average, about 60% of dust in the Minsk atmosphere is of transborder origin, while 40% is generated by sources lying at the Belarus territory. The atmosphere of Belsk experiences nearly the identical influence from national and foreign dust sources.

Acknowledgements

The NASA data on back trajectories of air masses²¹ were obtained by Tom Kucsera in the NASA Goddard Space Flight Center, Code 613.3, Greenbelt, MD 20771.

The NILU data on back trajectories of air masses²² were calculated by the Flextra model developed by Andreas Stohl (NILU) in cooperation with Gerhard Wotawa and Petra Seibert (Institute of Meteorology and Geophysics, Vienna) based on ECMWF (European

Centre for Medium Range Weather Forecast) meteorological data.

This work was supported in part by the International Science and Technology Centre (ISTC) (Project B-1063).

References

1. L.L. Ashbaugh, J. of Air Pollution Control Assessment **33**, No. 12, 1096–1098 (1983).
2. L.L. Ashbaugh, W.C. Malm, and W.Z. Sadeh, Atmos. Environ. **19**, No. 7, 1263–1270 (1985).
3. R.L. Poirot and P.R. Wishinski, Atmos. Environ. **20**, No. 18, 1457–1469 (1986).
4. P. Seibert, H. Kromp-Kolb, U. Baltensperger, D.T. Jost, M. Schwikowsky, A. Kasper, and H. Puxbaum, in: *Transport and Transformation of Pollutants in the Troposphere*, P.M. Borrell, P. Borrell, T. Cvitas, and W. Seiler, eds. (Academic Publishing, Den Haag, 1994), pp. 689–693.
5. A. Stohl, Atmos. Environ. **30**, No. 4, 579–587 (1996).
6. A. Rúa, E. Hernández, J. de las Parras, I. Martín, and L. Gimeno, J. Air and Waste Management Association **48**, No. 7, 838–845 (1998).
7. G. Wotawa, H. Kröger, and A. Stohl, Atmos. Environ. **34**, No. 7, 1367–1377 (2000).
8. A. Charron, H. Plaisance, S. Sauvage, P. Coddeville, J.C. Galoo, and R. Guillermo, Atmos. Environ. **34**, No. 19, 3665–3674 (2000).
9. F. Apadula, A. Gotti, A. Pignini, A. Longhetto, F. Rocchetti, C. Cassardo, S. Ferrarese, and R. Forza, Atmos. Environ. **37**, No. 18, 3757–3770 (2003).
10. L.Y.L. Lee, R.C.W. Kwok, Y.P. Cheung, and K.N. Yu, Atmos. Environ. **38**, No. 36, 7033–7040 (2004).
11. Yu.S. Balin and A.D. Ershov, Atmos. Oceanic Opt. **12**, No. 7, 592–599 (1999).
12. V. Matthias and J. Bosenberg, *EARLINET: A European Aerosol Research Lidar Network to Establish an Aerosol Climatology*, Report No. 348 of Max-Planck-Institute for Meteorology (Hamburg, 2003), 191 pp.
13. A. Chaikovsky, A. Bril, V. Barun, O. Dubovik, B. Holben, A. Thompson, Ph. Goloub, and P. Sobolewski, in: *Reviewed and Revised Papers Presented at the 22nd International Laser Radar Conference (ILRC 2004)* (Matera, Italy, 2004), pp. 345–348.
14. *Atmosphere. Reference Book* (Gidrometeoizdat, Leningrad, 1991), 509 pp.
15. V.A. Shnaidman, L.V. Berkovich, and O.V. Foskarino, Meteorol. Gidrol., No. 9, 98–107 (1987).
16. I.A. Businger, I.C. Wyngaard, G. Isume, and E.F. Bradly, J. Atmos. Sci. **28**, No. 2, 181–189 (1971).
17. V.E. Zuev and M.V. Kabanov, *Optics of Atmospheric Aerosol* (Gidrometeoizdat, Leningrad, 1987), 254 pp.
18. V. Vestreng, K. Breivik, M. Adams, A. Wagener, J. Goodwin, O. Rozovskaya, and J.M. Pacyna, *Inventory Review 2005, Emission Data reported to LRTAP Convention and NEC Directive, Initial review of HMs and POPs*, Technical Report MSC-W 1/2005, ISSN 0804-2446.
19. <http://webdab.emep.int/>
20. A. Stohl, Atmos. Environ. **32**, No. 6, 947–966 (1998).
21. <http://croc.gsfc.nasa.gov/aeronet/IMAGES>
22. <http://www.nilu.no/trajectories/files/datfiles/datfiles.cfm>